Modeling of Wavelength Conversion Using Switching Bistability in a Vertical Cavity Semiconductor Saturable Absorber

L. Mishra and P. K. Datta
Department of Physics, Indian Institute of Technology, Kharagpur, India
Email: {lokanath17, pkdatta.iitkgp}@gmail.com

R. Pradhan
Department of Physics, Midnapore College, West Bengal, India
Email: rajib.pradhan@gmail.com

***Abstract*—We have proposed a theoretical model to study bistable switching between two optical signals using a vertical cavity semiconductor saturable absorber (VCSSA) operating in reflection mode. The model is based on the carrier rate equation, which predicts cross-absorption phenomena within the absorber region. Simulations are carried out to investigate the effect of various cavity parameters on switching performance of the device. As an application, we have studied wavelength conversion of a 10Gb/s non-return-to-zero data signal, using the same model for bistable switching.**

***Index Terms*—optical bistability, bistable switching, cross-absorption modulation, wavelength conversion**

I. Introduction

All-Optical wavelength conversion is a more advances conversion technique in recent WDM network systems. The conversion process in general utilizes some nonlinear optical effects, which includes four wave mixing (FWM), cross-phase modulation (XPM) and cross-absorption modulation (XAM) to realize the wavelength conversion in some optical components like SOAs [1], [2] and nonlinear loop mirrors [3]. Also there are lots of experiments on wavelength conversion through XAM has been observed in many optical components like vertical cavity semiconductor saturable absorbers (VCSSAs) [4], [5] and electro-absorption modulators (EAMs) [6]. In this paper, we have developed a theoretical model to explain wavelength conversion process in a VCSSA, using bistability of the device.

A VCSSA has numerous applications in optical switching [7], [8] and all-optical signal regeneration [9], [10]. It is designed as a resonant Gires-Tournois interferometer with semiconductor multiple quantum well (MQWs) based absorption layers positioned between an asymmetric Fabry-Perot cavity. The device shows bistable characteristics by utilizing both nonlinear absorption and the dispersion of the MQWs within a feedback cavity. The dispersive bistability arises from the intensity dependence of refractive index [11]. Here, we have considered the combined effect of carrier dependence of absorption coefficients and refractive index change to study bistability in our model. This paper is organized as follows: In section-II, we have studied numerically the bistability switching between two optical signals at different wavelengths based on the XAM in the MQWs structures. In section-III, we have studied the wavelength conversion process in a VCSSA, using the results obtained from the above nonlinear model and the last section concludes.

II. Bistable Switching

A. Bistable Characteristics of the Nonlinear Device

A VCSSA exhibits high nonlinear characteristics. The maximum nonlinearity of the VCSSA is achieved by the combined effect of the asymmetric Fabry-Perot (FP) cavity and the MQWs [7]. An asymmetric Fabry–Perot cavity is usually formed by the semiconductor/dielectric distributed Bragg reflectors (DBR) with less reflective front mirror (R_t) and a highly reflective back mirror (R_b).

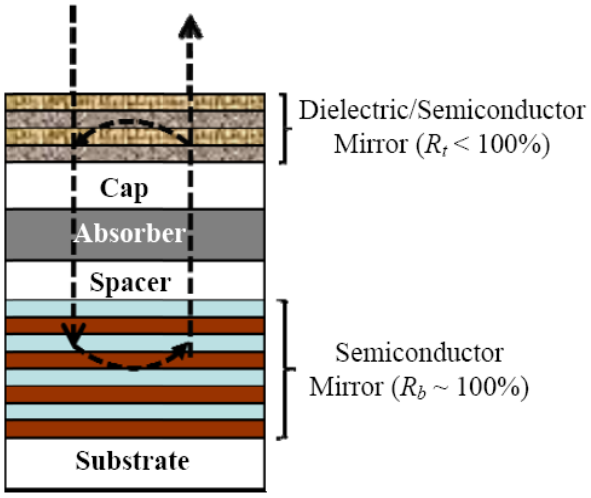

Figure 1. Schematic structure of a nonlinear VCSSA

Manuscript received May 21, 2014; revised October 30, 2014.

doi: 10.12720/ijeee.3.5.396-401

The DBR mirrors are consists of alternating layers of high and low refractive index materials, each of thickness equals to $\lambda/4$, where λ is the central wavelength of the DBR stop band. The DBR reflectivity depends on the number of piled layers and the difference in the refractive index (Δn) of the adjacent layers. Usually the devices were grown by solid-source molecular beam epitaxy on an n-type InP substrate. The schematic of the device structure is shown in Fig. 1. It comprises a bottom DBR, an InP spacer layer, the absorber region (MQWs), an InP cap layer, and a top DBR [12]. The DBR layers and the QW layers are chosen to be same semiconductor materials for the requirement of lattice matching. In our model, we have considered an InGaAs/InP based MQWs, to operate the device near 1550nm. Both cap and spacer layers allow multiple resonances of the device within the communication wavelength range. In order to decrease the absorber recovery time, the active region is usually irradiated with the proper dose of heavy ions. The irradiated sample is then coated with few layers of SiO_2/TiO_2 providing the specified top mirror reflectivity at the resonance wavelength of the device. The top mirror reflectivity R_t determines the amount of light entering the saturable absorber and therefore controls the nonlinear reflectivity [13]. For such a device the spectral dependent power reflectivity can be calculated by using the standard formula for a FP-cavity incorporating the losses [8].

$$R=\frac{R_t+R_b\,e^{-2\alpha D}-2\sqrt{R_tR_b}e^{-\alpha D}\cos\left(\phi_{rt}\right)}{1+R_tR_b\,e^{-2\alpha D}-2\sqrt{R_tR_b}e^{-\alpha D}\cos\left(\phi_{rt}\right)} \tag{1}$$

where, αD is the total absorption within the VCSSA cavity, which can be expressed as

$$\alpha D=\alpha_{ns}d+\frac{\alpha_0 d_1}{1+P_c/P_{sat}} \tag{2}$$

where, d is the physical length of the micro-cavity resonator which includes the cap layer, the active region (MQWs), and the spacer layer, d_1 is the total width of the QWs, α_0 is the low power absorption coefficient, and α_{ns} is the nonsaturable part of the absorption. ϕ_{rt} is the round-trip phase of the optical field within the cavity and $\phi_{rt}=\phi_{Linear}+\phi_{Nonlinear}$ [8]. Where ϕ_{Linear} is the actual phase associated with the field within the cavity and is equal to $2m\pi$ (considering resonance at low input power), m is any positive integer. The nonlinear contribution of the phase arises from the photo induced change in carrier density. The light intensity within the cavity induces an index change, which introduce a phase change: $\phi_{Kerr}=4\pi d_1\left(\Delta n\right)/\lambda_{work}$, called the phase due to *Kerr-nonlinearity*. Where Δn is the change in material refractive index, that varies with intra-cavity intensity as $\Delta n=n_2I_c$, with n_2 is the third-order nonlinear optical property of the medium. Defining $\Delta n=\Delta n_{\max}\left(\frac{P_c/P_{sat}}{1+P_c/P_{sat}}\right)$, with $\Delta n_{max}=n_2I_{sat}=n_{2s}$, we have the phase-change equals to:

$$\phi_{Kerr}=\frac{4\pi n_{2s}d_1}{\lambda_{work}}\left[\frac{P_{cs}}{\left(1+P_{cs}\right)}\right] \tag{3}$$

$P_{cs}=P_c/P_{sat}$, where P_c and P_{sat}, are respectively the cavity power and the saturation power of the nonlinear device. Further, $\phi_{shift}=4\pi nd\left(\frac{1}{\lambda_{work}}-\frac{1}{\lambda_{res}}\right)$ is the extra phase detuning of the optical field, when the device operated at a wavelength other than the resonant wavelength of the cavity. However, the total power absorption introduces some thermal effects, because of which the resonance shifts towards higher wavelength side due to increase in effective cavity length. This results in some additional phase to the optical field. Thus, the total corrected phase now becomes

$$\phi_{rt}=\frac{4\pi n_{2s}d_1}{\lambda_{work}}\left[\frac{P_{cs}}{\left(1+P_{cs}\right)}\right]+4\pi nd\left(\frac{1}{\lambda_{work}}-\frac{1}{\lambda_{res}+\Delta\lambda}\right) \tag{4}$$

where $\Delta\lambda=\left(d\lambda_{res}/dT_{act}\right)R_{th}P_c\alpha D$ is the shift of the resonance wavelength due to thermal effects [14]. R_{th} is the effective thermal resistance and $d\lambda_{res}/dT_{act}$ is the rate at which the cavity resonant wavelength changes with actual temperature of the device. The thermal effect in the device persists in a time scale of few micro-seconds. For device characterization, we usually considered the CW approximation. Thus, the shifting $\Delta\lambda$ due to thermal effects has to be calculated for each values of the input power. But, this approximation is not acceptable for an optical signal having pulse width in the pico-second order. For such a case $\Delta\lambda$ is considered to be constant, and it assumes the value corresponding to the pulse peak power (i.e. $\Delta\lambda=\Delta\lambda(P_{in}^{MAX})$). However, this shifting will not affect to the temporal characteristics of the signal. All simulated results that have been presented in this paper are calculated assuming $\Delta\lambda=\Delta\lambda(P_{in}^{MAX})$. The length-averaged power inside the cavity can be expressed as [8]

$$P_c=\frac{\left(1-R_t\right)\left(1-e^{-\alpha D}\right)\left(1+R_be^{-\alpha D}\right)P_{in}}{\alpha D\left(\left(1-\sqrt{R_tR_b}e^{-\alpha D}\right)^2+4\sqrt{R_tR_b}e^{-\alpha D}\sin^2\left(\phi_{rt}/2\right)\right)} \tag{5}$$

The power reflected from a VCSSA, follows the expression

$$P_{ref}=R\left(\phi_{rt},\alpha\right)P_{in} \tag{6}$$

where, P_{in} and P_{ref} are the incident and reflected power of the optical signal, respectively. It is observed from eqn. (6) that the reflected power, which depends on the reflectivity of the device, is a function of both phase and total absorption. The above two parameters (α and ϕ_{rt}) are strongly depend on the power inside the cavity, which is controlled by the feedback cavity through top mirror reflectivity. The reflected power as a function of the input power at 1550nm for different top mirror reflectivities has shown in Fig. 2. The plot shows that, a clockwise bistability with narrow bistable loop and low threshold power could be obtained for a small value of top mirror

reflectivity (R_t). The device parameters used in our simulations are given in Table I.

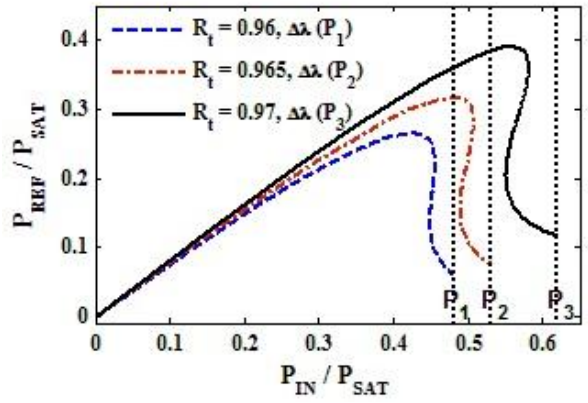

Figure 2. Normalized incidence power vs. output reflected power at 1550 nm for different values of top mirror reflectivity.

TABLE I. QUANTUM WELLS PARAMETERS

Symbols	Parameters	Values	Units
d	Cavity Length	3λ/2n	
d_1	Length of the active region	0.3	*μm*
a_0	Low power absorption coefficient	10^6	m^{-1}
$a_{ns}d$	Nonsaturable Absorption	0.0125	
n_{2s}	Saturated nonlinear index	-0.025	
P_{sat}	Saturation Power	40	*mW*
R_{th}	Effective thermal resistance of the micro-cavity	3000	*K/W*
λ_{res}	Micro-cavity resonance wavelength	1550	*nm*
$(d\lambda/dT)_{res}$	Rate of change of resonance wavelength with temperature	0.1	*nm/K*
R_b	Bottom mirror reflectivity	0.995	
n	Average R.I. of MQWs	3.56	

B. Switching Bistability

Bistable switching between two optical signals, each at different wavelengths were studied first time using a Fabry-Perot semiconductor laser amplifier (FPSLA) working in transmission mode [15]. Later on some experiments were carried out to study the switching properties using some devices like semiconductor laser amplifier [16] and distributed feedback semiconductor optical amplifier (DFBSOA) [17]. In this paper, we have demonstrated bistability switching between two optical signals using a passive device like VCSSA. In this section, we have studied the switching of a signal beam by another control beam fixed at the cavity resonance wavelength of 1550nm, using bistability of the device. To study the switching behavior of the device, we have fixed the signal beam at a wavelength other than the cavity resonant wavelength with very low input power. On gradually increasing the input power of the control beam, the carrier concentration within the cavity increases, this modifies the absorption and refractive index of the saturable absorber. The rate at which the carrier density (N) changes within the absorber region is given by

$$\frac{dN}{dt} = \frac{\alpha(\omega_c)P_c(\omega_c)}{\hbar\omega_c} + \frac{\alpha(\omega_s)P_c(\omega_s)}{\hbar\omega_s} - \frac{N}{\tau} \tag{7}$$

where, ω_c and ω_s are the angular frequencies of the control and signal beam, respectively and $\alpha(\omega_c)$ and $\alpha(\omega_s)$ are their corresponding absorption coefficients. τ is the carrier recombination time. For a fast absorber and under continuous wave approximation, we have $dN/dt = 0$. This implies

$$N = \left(\frac{\alpha P_c(\omega_c)}{\hbar\omega_c} + \frac{\alpha P_c(\omega_s)}{\hbar\omega_s} \right) \tau \tag{8}$$

here we have considered the absorption (i.e. $\alpha(\omega_c) = \alpha(\omega_s) = \alpha$), is spectral independent within a small range of detuning $\Delta\lambda \sim 10\,\text{nm}$. Now these carriers modulate the absorption coefficient of the nonlinear device according to [18]

$$\alpha_{sat} = \frac{\alpha_0}{1 + N/N_{sat}} = \frac{\alpha_0}{1 + P_{ct}/P_{sat}} \tag{9}$$

where, $N_{sat}\left[= \frac{\alpha P_{sat}}{\hbar\omega}\tau \right]$ is the saturated carrier density and $P_{ct} = P_c(\omega_c) + P_c(\omega_s)$ is the total power within the cavity. Similarly the phase due to Kerr-nonlinearity will be modified by

$$\phi_{Kerr} = \frac{4\pi n_{2s} d_1}{\lambda_i} \left(\frac{P_{ct}/P_{sat}}{1 + P_{ct}/P_{sat}} \right) \tag{10}$$

where i = c or s, is the index for control and signal beam, respectively. The change in phase due to Kerr-nonlinearity will shift the cavity resonance towards the shorter wavelength regime (blue-shift), whereas a red-shift of cavity resonance will take place due to the thermal effect. The combined phase effect together with the total absorption is responsible for the change in reflectivity of the device. This results in change of output powers of both the beam. The output of the signal and control beam powers follows the equations

$$P_{ref,1} = R(\phi_1, \alpha) P_{in,1}$$

$$\text{and} \qquad P_{ref,2} = R(\phi_2, \alpha) P_{in,2} \tag{11}$$

The simulated result as plotted in Fig. 3(a) and Fig. 3(b) are respectively, shows the reflected power of both control and signal beam as a function of the control beam input power $(P_{in,1})$, and in presence of the signal beam at four different wavelengths. It is observed from the plot that, wider bistable loop with high extinction ratio (ER) could be obtained for the signal beam at 1551nm.

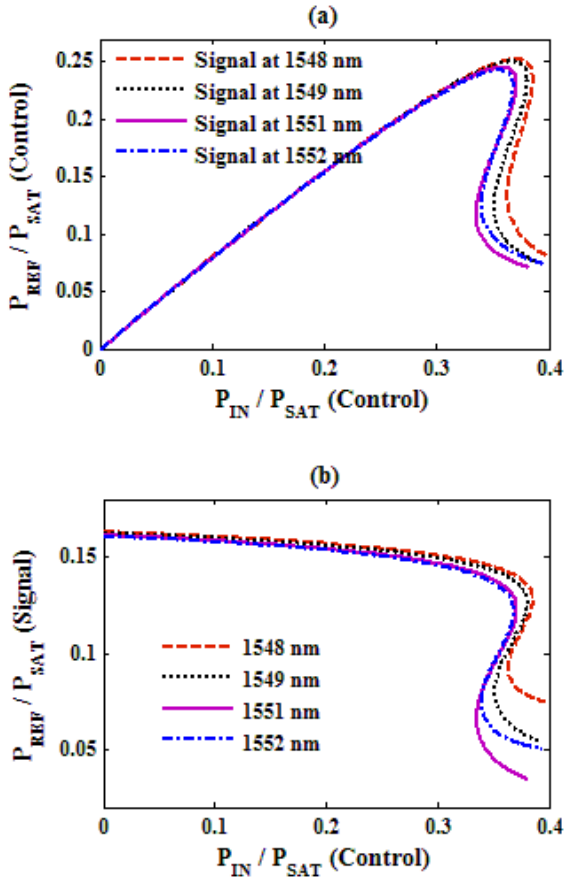

Figure 3. (a) Normalized incidence power vs. reflected power of the control beam in presence of signal beam at four different wavelengths, (b) Reflected signal beam power as a function of input control beam power. R_t=0.97, λ_c=1550nm, P_{IN} (Signal)=0.2P_{SAT}

C. *Effect of $\alpha_0 d_1$ on Bistability*

Fig. 4 shows the simulated input/output curve for a signal beam at 1551nm, with small-signal absorption as a parameter. The curves show that the threshold power increases with an increase in small signal absorption. Also the bistable loop is wider in this case, but the high value of absorption is not desirable, since it increases the temperature of the device.

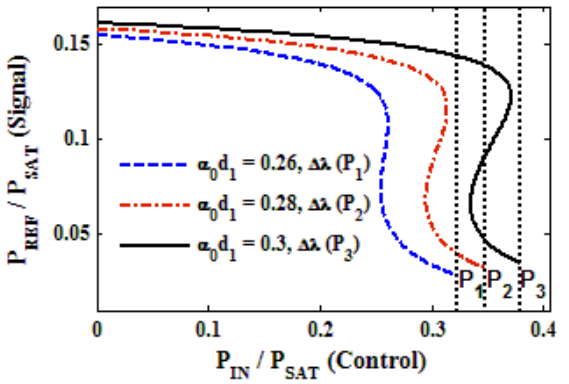

Figure 4. Normalized incidence control beam power vs. reflected signal beam power for different values of small-signal absorption, λ_S=1551nm, P_{IN} (Signal)=0.2P_{SAT}

III. Wavelength Conversion

The same model has been used to study wavelength conversion in a VCSSA based on our previous results of bistable switching, and the schematic of the model is shown in Fig. 5. The probe beam at λ_2 from the CW laser source and the data signal at λ_1 will be sent simultaneously to the VCSSA through the input end of the circulator, and the converted probe signal at λ_2 will be collected from the output terminal of the circulator. The low power spectral reflectivity of the device is shown in the inset of Fig. 6 (black dotted line). To study wavelength conversion between two optical signals, we have used a pump signal at a wavelength exactly matching the cavity resonance of 1550nm (black arrow). The pump beam, which carries the signal, is modulated with a 10GB/s pseudo random binary sequence (2^7-1) non-return-to-zero (NRZ) data signal with an extinction ratio (ER) of 12.26dB. A CW diode laser at 1551nm is used as a probe signal (gray arrow) with an input power of $P_{in,2}=0.25P_{sat}$. It is clear from Fig. 6 that, the reflected power of the probe beam is maximum ('ON' state) at low input power of the pump signal ('OFF' state).

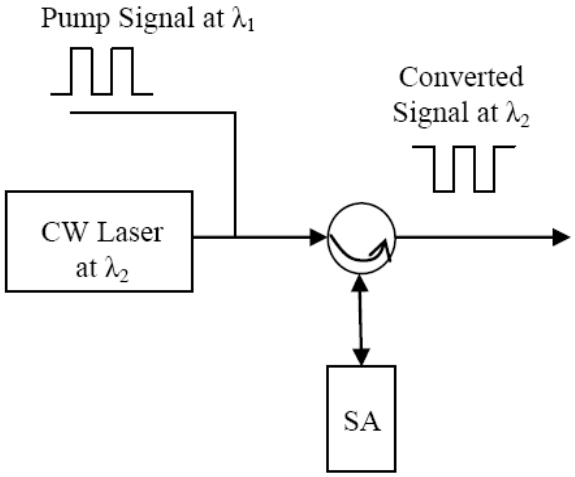

Figure 5. Schematic of the model used for wavelength conversion

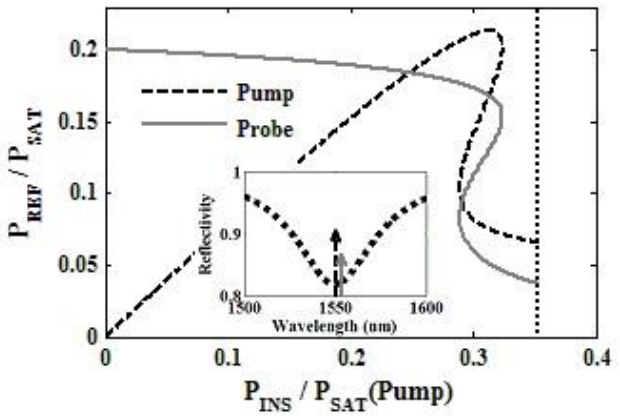

Figure 6. Normalized incidence pump beam power vs. output reflected power (both pump and probe beam). R_t = 0.97, P_{IN} (Signal) = 0.25 P_{SAT}

With gradually increasing the power of the pump beam, the absorption within the quantum well decreases, and simultaneously the intracavity intensity increases, results in a further decrease in absorption. This continues until the reflectivity jumps discontinuously to a minimum value for a given switched down power ($P_{\downarrow}$), where both pump and probe beam have their minimum reflected power (as shown in Fig. 6). The output of the probe beam decreases with further increasing input pump power. In our case we have chosen the input power of the pump beam corresponding to the 'ON' state is slightly greater than the downward threshold power ($P_{\downarrow}$), for which the output of the probe beam is minimum ('OFF' state). Fig. 7 shows the plot of the incident data signal at 1550nm and the converted probe signal at 1551nm. It is clear from our simulation that the converted signal is of an inverting type with a calculated ER of 7.38dB.

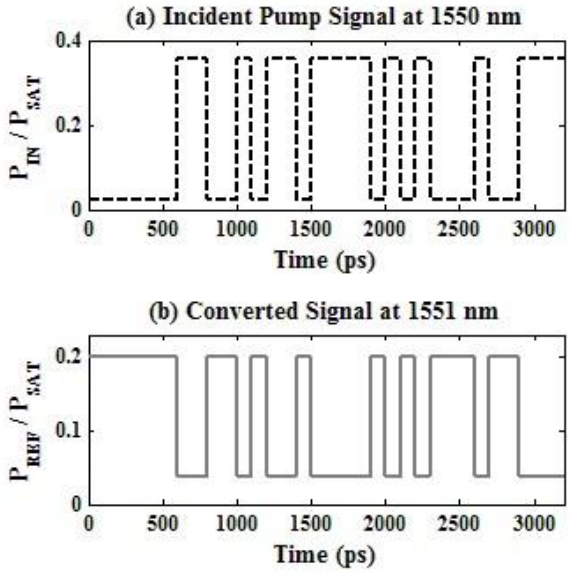

Figure 7. Plot of (a) input data signal and (b) converted probe signal as a function of time (ps).

IV. Conclusion

Bistability switching between two optical signals of different wavelengths has been studied theoretically in a passive VCSSA, based on the XAM within the MQWs. Clockwise switching with wider bistable loop and high extinction of the optical signal could obtained by properly selecting the operating wavelength and the cavity parameters. Simultaneously, wavelength conversion in a VCSSA has been studied theoretically by utilizing the same model of bistable switching. We observed an extinction ratio of 7.38dB for the converted signals at 1551nm, against a 10Gb/s NRZ data signal at 1550 and an extinction of 12.26dB. Now a day VCSSA's are available with a carrier recombination time of the order of few ps (~1ps), which could be used for wavelength conversion of high bit-rate signals (upto 80Gb/s or more). The operation could be in principle extended to a broad wavelength regime, which is desirable for WDM signal transmission systems. The most important aspects of a VCSSA used for wavelength conversion is due to its small size, easy to fabricate and does not require any biasing for its operation.

References

[1] O. Napolea, S. Riberio, M. G. Cristiano, and C. Evandro, "Wavelength converters characterization based on four-wave mixing and cross-gain modulation using semiconductor optical amplifier of diverse cavity length," *Microwave and Optical Technology Letters*, vol. 50, no. 12, pp. 3246-3251, Sep. 2008.

[2] D. F. Geraghty, *et al.*, "Wavelength conversion for WDM communication systems using four-wave mixing in semiconductor optical amplifiers," *IEEE Journal of Selected Topics in Quantum Electronics*, vol. 3, no. 5, pp. 1146-1155, Oct. 1997.

[3] J. Liu, *et al.*, "Degenerate four-wave mixing based all-optical wavelength conversion in a semiconductor optical amplifier and highly-nonlinear photonic crystal fiber parametric loop mirror," *Optics Communications*, vol. 281, no. 21, pp. 5415-5419, Nov. 2008.

[4] T. Akiyama, M. Tsuchiya, K. Igarashi, and T. Kamiya, "Wavelength conversion (~14nm) of 1-Gbit/s signal by a low-temperature grown asymmetric fabry-perot all-optical device," in *Proc. CLEO'98*, May 1998, pp. 476-477.

[5] C. Porzi, M. Guina, L. Orsila, A. Bogoni, and L. Poti, "Simultaneous dual-wavelength conversion with multiresonant saturable absorption vertical-cavity semiconductor gate," *IEEE Photonics Tech. Lett.*, vol. 20, no. 7, pp. 499-501, Apr. 2008.

[6] N. Cheng, and J. C. Cartledge, "Measurement-Based model for cross-absorption modulation in an MQW electro-absorption modulator," *IEEE J. of Lightwave Technology*, vol. 22, no. 7, pp. 1805-1810, Jul. 2004.

[7] Y. Tang, A. Siahmakoun, G. Sergio, M. Guina, and M. Pessa, "Optical switching in a resonant fabry-perot satururable absorber," *J. of Opt. A: Pure Appl. Opt*., vol. 8, no. 11, pp. 991-995, Oct. 2006.

[8] L. Mishra, R. Pradhan, and P. K. Datta, "Modeling of two wavelength switching using a reflective vertical cavity semiconductor saturable absorber," *Opt. Commun*., vol. 331, pp. 267-271, Jun. 2014.

[9] L. Mishra, *et al*., "Phase-Response characterization of semi-conductor saturable absorber for applications in nonlinear optical signal processing and phase-modulated signals regeneration," in *Proc. SPIE, Optical Components and Material VIII*, Feb. 2011, vol. 7934, pp. 79340E1-79340E7.

[10] R. Pradhan, L. Mishra, K. Hussain, S. Saha, and P. K. Datta, "All-Optical 2R regeneration with contrast enhancement in a reflective vertical cavity quantum-wells saturable absorber," *J. Opt. Commun. Netw*., vol. 5, no. 5, pp. 1-8, May 2013.

[11] N. Peyghambarian and H. M. Gibbs, "Optical nonlinearity, bistability, and signal processing in semiconductors," *J. Opt. Soc. Am. B*, vol. 2, no. 7, pp. 1215-1227, Jul. 1985.

[12] J. Grym, *Semiconductor Technology*, InTech Publisher, 2010, ch. 14, pp. 321-346.

[13] L. R. Brovelli, U. Keller, and T. H. Chiu, "Design and operation of antiresonant fabry-perot saturable semiconductor absorbers for mode-locked solid-state lasers," *J. Opt. Soc. Am. B*, vol. 12, no. 2, pp. 311-322, Feb. 1995.

[14] D. Massoubre, J. L. Oudar, A. O'Hare, M. Gay, and L. Bramerie, "Analysis of thermal limitations in high-speed microcavity saturable absorber all-optical switching gates," *IEEE J. of Lightwave Technology*, vol. 24, no. 9, pp. 3400-3408, Sep. 2006.

[15] H. Kawaguchi, H. Tani, and K. Inoue, "Optical bistability using a fabry-perot semiconductor-laser amplifier with two holding beams," *Optics Letters*, vol. 12, no. 7, pp. 513-515, Jul. 1987.

[16] A. Hurtado and M. J. Adams, "Two-Wavelength switching with 1550nm semiconductor laser amplifiers," *J. Optical Networking*, vol. 6, no. 5, pp. 434-441, May 2007.

[17] A. Hurtado, A. Gonzalez-Marcos, J. A. Martin-pereda, and M. J. Adams, "Two-Wavelength switching with a distributed-feedback semiconductor optical amplifier," *IEE Proc.-Optoelectronics*, vol. 153, no. 1, pp. 21-27, Feb. 2006.

[18] S. H. Park, *et al.*, "Measurements of room temperature band-gap-resonant optical nonlinearities of GaAsl AiGaAs multiple quantum wells and bulk GaAs," *Appl. Phys. Lett.*, vol. 52, no. 15, pp. 1201-1203, Apr. 1985.

Lokanath Mishra received his M.Sc. degree in physics from Sambalpur University, Odisha, India, in 2004. He is currently working toward the Ph.D. degree at IIT, Kharagpur, India. During 2010, he was a visiting research scholar at the Center of Excellence for Information, Communication and Perception Engineering, Scuola Superiore Sant'Anna, Pisa, Italy. His current research interest is focused on modeling and characterization of vertical cavity semiconductor saturable absorbers for use in optical communication.

Rajib Pradhan received his M.Sc. degree in physics from Vidyasagar University, West Bengal, India, in 2001. He joined the Department of Physics Midnapore College, India, in 2006 as an Assistant Professor and is currently pursuing research work in collaboration with IIT, Kharagpur, India. His areas of interest are vertical cavity semiconductor saturable absorbers and SOA-based all-optical devices.

Prasanta Kumar Datta received his Ph.D. degree from Burdwan University, India, in 1994 and worked at Pavia University, Italy, and Strathclyde University, Scotland, for his postdoctoral work on cascaded quadratic processes before joining IIT, Kharagpur, India, in 2000. He has developed a laboratory for the study of ultrafast nonlinear optics with sponsored projects from various agencies. His present interest is in i) ultrafast nonlinear optics, ii) optical parametric amplifiers and oscillators, and iii) SOA and semiconductor-saturable-absorber-based photonic devices. He has 55 journal publications in his credit and guided 4 Ph.Ds.